

## Cold and intense OH radical beam sources

Ludger Ploenes<sup>1</sup>, Dominik Haas<sup>1</sup>, Dongdong Zhang<sup>1</sup>, Sebastiaan Y. T. van de Meerakker<sup>1</sup>, and Stefan Willitsch<sup>1</sup>

Citation: *Review of Scientific Instruments* **87**, 053305 (2016); doi: 10.1063/1.4948917

View online: <http://dx.doi.org/10.1063/1.4948917>

View Table of Contents: <http://aip.scitation.org/toc/rsi/87/5>

Published by the *American Institute of Physics*

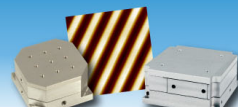
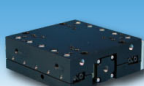
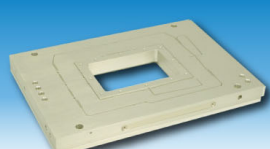
---

### Articles you may be interested in

[A new high intensity and short-pulse molecular beam valve](#)

*Review of Scientific Instruments* **84**, 023102023102 (2013); 10.1063/1.4790176

---



Nanopositioning Systems      Micropositioning      AFM & SPM      Single molecule imaging

## Cold and intense OH radical beam sources

Ludger Ploenes,<sup>1,a)</sup> Dominik Haas,<sup>2,a)</sup> Dongdong Zhang,<sup>2,b)</sup>  
 Sebastiaan Y. T. van de Meerakker,<sup>1</sup> and Stefan Willitsch<sup>2,b)</sup>

<sup>1</sup>*Institute for Molecules and Materials, Radboud University, Heijendaalseweg 135,  
 6525 AJ Nijmegen, The Netherlands*

<sup>2</sup>*Department of Chemistry, University of Basel, Klingelbergstrasse 80,  
 4056 Basel, Switzerland*

(Received 16 February 2016; accepted 24 April 2016; published online 18 May 2016)

We present the design and performance of two supersonic radical beam sources: a conventional pinhole-discharge source and a dielectric barrier discharge (DBD) source, both based on the Nijmegen pulsed valve. Both designs have been characterized by discharging water molecules seeded in the rare gases Ar, Kr, or Xe. The resulting OH radicals have been detected by laser-induced fluorescence. The measured OH densities are  $(3.0 \pm 0.6) \times 10^{11} \text{ cm}^{-3}$  and  $(1.0 \pm 0.5) \times 10^{11} \text{ cm}^{-3}$  for the pinhole-discharge and DBD sources, respectively. The beam profiles for both radical sources show a relative longitudinal velocity spread of about 10%. The absolute rotational ground state population of the OH beam generated from the pinhole-discharge source has been determined to be more than 98%. The DBD source even produces a rotationally colder OH beam with a population of the ground state exceeding 99%. For the DBD source, addition of O<sub>2</sub> molecules to the gas mixture increases the OH beam density by a factor of about 2.5, improves the DBD valve stability, and allows to tune the mean velocity of the radical beam. *Published by AIP Publishing.* [<http://dx.doi.org/10.1063/1.4948917>]

### I. INTRODUCTION

The high reactivities of free radicals make them the major players in a wide range of chemical processes and important reaction agents in atmospheric, interstellar, combustion, and biological environments. Laboratory studies of free radicals demand for an efficient, reliable, and controllable method to generate free radicals as a base for characterizing their fundamental properties.<sup>1</sup>

The molecular beam technique is one of the best established methods to generate free radicals under well-defined conditions.<sup>2</sup> This approach provides the collision free environment for the study of radicals in which directed beams can be produced with well defined translational energies. The use of a supersonic expansion in which a high pressure of gas issues from a small-diameter nozzle ensures that cooling of the internal degrees of freedom of the radicals takes place and rotational temperatures of <10 K are easily achieved. This means that only the lowest rotational and fine-structure levels of the radical will be populated, allowing for a high degree of state selection. Many experiments in physics and chemistry benefit from or even rely on atomic and molecular beams, e.g., tests of fundamental aspects of quantum mechanics,<sup>3</sup> molecular reaction dynamics,<sup>4–6</sup> and manipulation of molecules.<sup>7,8</sup>

One of the most widely studied free radical species is hydroxyl OH, which holds an essential role in biochemical, interstellar, atmospheric, and combustion science.<sup>9–12</sup> Three major approaches have been used to generate OH radicals with the molecular beam technique: photolysis,<sup>13</sup> chemical

reactions,<sup>14,15</sup> and electrical discharge.<sup>16–18</sup> Of these, the discharge method is the most cost-efficient, simplest, and the most broadly applicable.

A special form of discharge is the dielectric barrier discharge (DBD),<sup>19</sup> where the discharge takes place across a dielectric material between high voltage electrodes. The self-limiting current, due to charge saturation in the dielectric barrier, leads to an overall gentler discharge process which finally results in a lower temperature of the generated plasma. DBDs are widely used in industrial applications like the production of ozone,<sup>20</sup> the reduction of environmental pollution,<sup>21</sup> and in UV-light generation.<sup>22</sup> The effectiveness of this technique for the production of high-quality supersonic beams of radicals has been demonstrated by Even *et al.*<sup>23</sup>

In this paper, we present the combination of discharge methods with a Nijmegen pulsed valve (NPV) to generate radical beams. The NPV has been shown to be able to produce temporally short molecular beam pulses with high particle densities.<sup>24,25</sup> The objective of the present work is the production of cold and intense radical beams benefiting from these features of the NPV. For direct comparison of conventional discharge and DBD methods, a pinhole-discharge and a DBD source have been combined with a NPV for the generation of OH radicals by the dissociation of H<sub>2</sub>O molecules. Here, we give a full characterization and direct comparison of both discharge sources in view of the experimental parameters which are relevant for molecule-deceleration and trapping experiments,<sup>7</sup> including the temporal profile, rotational state distribution, and density of the radical beam. Furthermore, we demonstrate that the addition of O<sub>2</sub> to the discharged gas mixture can increase the radical density in the DBD source and tune the mean velocity of the radical beam.

<sup>a)</sup>L. Ploenes and D. Haas contributed equally to this work.

<sup>b)</sup>Authors to whom correspondence should be addressed. Electronic addresses: dongdong.zhang@unibas.ch and stefan.willitsch@unibas.ch

## II. EXPERIMENTS

### A. Discharge sources

The pinhole-discharge source is based on the design of Lewandowski *et al.*<sup>18</sup> A schematic of the pinhole-discharge assembly together with the NPV can be found in Figure 1. The discharge takes place between two stainless steel electrodes, which are electrically insulated from each other and from the valve body by three Macor® plates. In our experiments, typically a voltage difference of 900 V between the electrodes is enough to produce stable discharges. The plate stack is mounted directly on top of the NPV body and features a 60° cone for the collimation of the molecular beam.<sup>26</sup>

The DBD source is modeled after the design introduced by Even *et al.*,<sup>23</sup> adapted to the NPV. Details of our DBD valve are shown in Figure 2. The discharge takes place along the inner surface of the dielectric material piece between the DBD electrode and the stainless steel body of the valve. The DBD is initiated by an alternating-current high-voltage pulse with a fixed frequency of around 1 MHz and an amplitude of about 4 kV directly applied to the DBD electrode. The pulse duration can be controlled by an external trigger pulse. The opening angle of the DBD nozzle orifice is 50°.

### B. Experimental setup

Both discharge sources have been characterized using the experimental setup shown in Figure 3. The discharge source is mounted on a xyz-translation stage inside a vacuum chamber, which is pumped by an 1000 l s<sup>-1</sup> turbo molecular pump. The NPV is operating at 10 Hz and creates a short pulse of a few tens of μs duration.<sup>24</sup> Each measurement is initiated by the trigger of the opening of the NPV, leading to the expansion of typically one percent of H<sub>2</sub>O seeded in a carrier gas (Ar, Kr, or Xe). The water molecules are dissociated during discharging and cooled by a supersonic expansion into high vacuum right afterwards. Typically, a stagnation pressure of 2.5 bars seeded

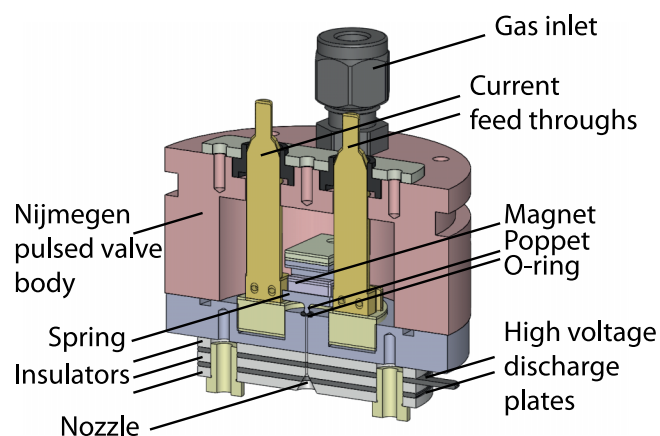


FIG. 1. Schematic illustration of the pinhole-discharge valve. The nozzle diameter is 0.5 mm. The thickness of the discharge plates and the insulators is 0.7 mm and 2.3 mm, respectively. The electrode and the insulator closest to the valve have a 0.5 mm diameter hole to match the valve nozzle. The conical orifice of the nozzle starts from the middle point of the second insulator and features a 60° opening angle. The H<sub>2</sub>O molecules are dissociated into OH radicals between the two high-voltage plates. See text for details.

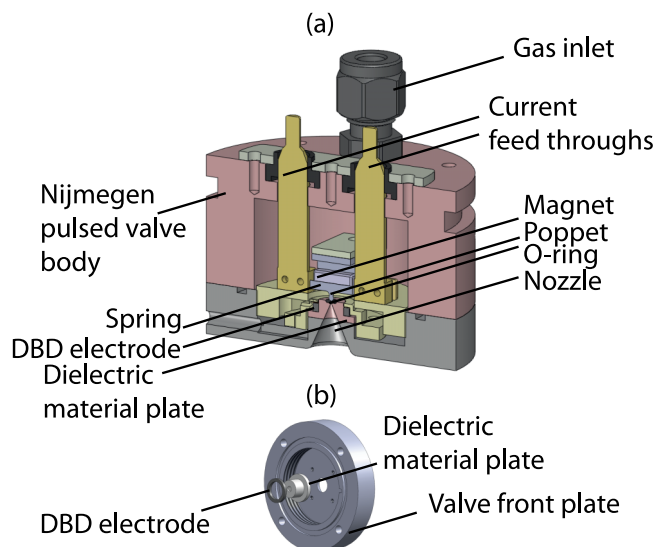


FIG. 2. (a) Schematic illustration of the DBD valve. The DBD electrode is a ring with an inner diameter of 9 mm, an outer diameter of 12 mm, and a thickness of 2 mm. The diameter of the nozzle is 0.3 mm. The conical orifice starts from a 0.3 mm diameter hole in the dielectric material plate and joins smoothly with the front plate of the valve to form a 50° opening angle. The discharge takes place along the surface of the dielectric material plate between the DBD electrode and the grounded valve body. (b) The details of the DBD setup. See text for details.

with water vapor pressure at room temperature is used. The pressure in the chamber during the operation of the valve is kept at around  $1.5 \times 10^{-5}$  mbar. Finally, the radicals are detected by laser-induced fluorescence (LIF) with an excitation-laser wavelength centered at 282 nm.<sup>16-18</sup>

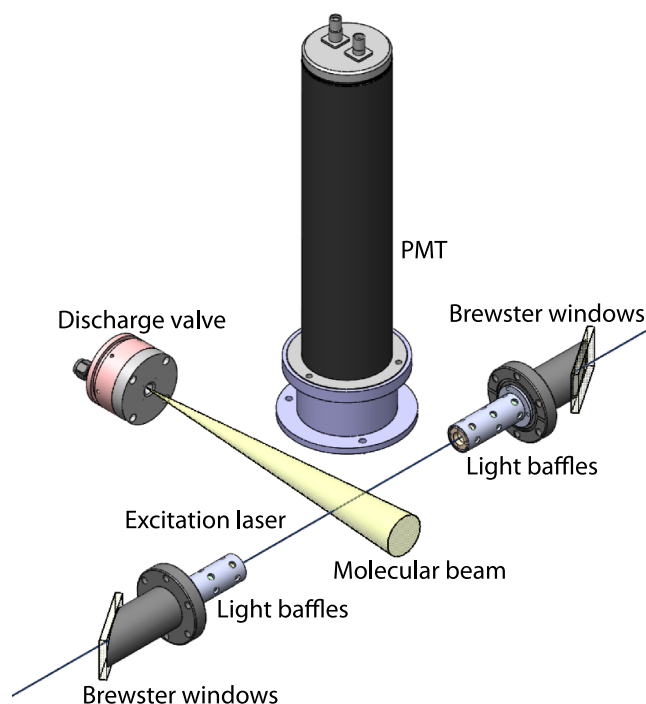


FIG. 3. Experimental setup for the characterization of both discharge sources. The light baffles have 3 mm diameter holes which define the probe beam diameter. The OH molecules are detected 5 cm downstream from the nozzle by laser-induced fluorescence (see text).

The excitation-laser beam enters and exits the vacuum chamber through a series of light baffles as shown in Figure 3 to suppress stray light. The excitation laser intersects the molecular beam perpendicularly 5 cm downstream from the nozzle. After their generation, OH molecules in the ground state  $X^2\Pi(v=0)$  are excited to the first excited electronic state  $A^2\Sigma(v=1)$ , where  $v$  denotes the vibrational quantum number. The 282 nm laser radiation is generated by the output of a frequency-doubled dye laser pumped by a Nd:YAG laser. The output energy is 10.0 mJ/pulse with a pulse duration of 10 ns. We find that 1.5 mJ/pulse is enough to saturate the OH X–A transition. Off-resonance fluorescence from the  $A^2\Sigma(v=1)$ – $X^2\Pi(v=1)$  transition with a wavelength of 313 nm is collected by a UV lens (50.8 mm diameter and 50 mm focal length) and detected by a calibrated photomultiplier tube (PMT) (Electron Tubes B2/RFI, 9813 QB). To further eliminate stray light, either from the excitation laser or from the discharge process, two interference filters and one dichroic mirror centered around the detection wavelength are used. Successful detection of OH has been confirmed through the observation of the fluorescence lifetime of  $717 \pm 18$  ns of the excited state as shown in Figure 4. The data points represent averages over 50 experimental cycles to improve the signal-to-noise ratio.

### III. RESULTS AND DISCUSSION

#### A. Pinhole-discharge source

The results of the characterization of the pinhole-discharge valve using three different carrier gases are summarized in Table I and are discussed in the following.

##### 1. OH beam profile

To measure the temporal profile of the OH beam, the LIF signal was recorded at varying trigger delays between

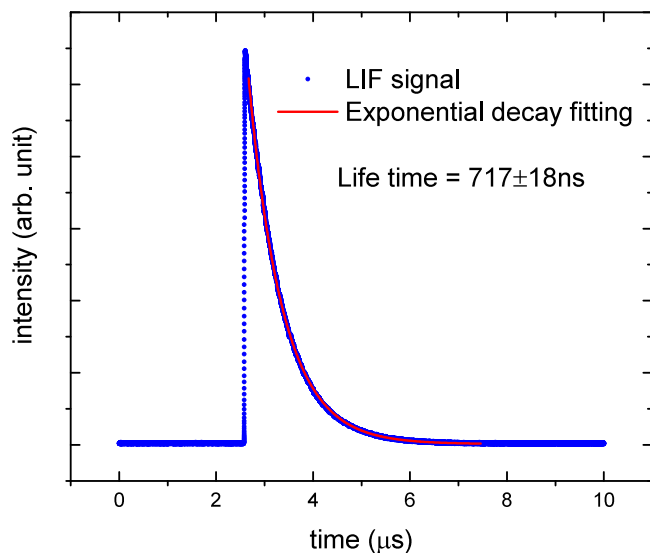


FIG. 4. Laser-induced fluorescence (LIF) signal of the OH radicals. The fitted lifetime of  $717 \pm 18$  ns agrees with previous results.<sup>27,28</sup>

TABLE I. OH radical beam properties generated from the pinhole-discharge source.

Carrier gas	Mean velocity /ms <sup>-1</sup>	Velocity spread (FWHM) (%)	Population in rotational ground state (%)	Density $\times 10^{11}$ /cm <sup>-3</sup>
Ar	$670.5 \pm 6.3$	$(9.8 \pm 0.5)$	>98	$3.0 \pm 0.6$
Kr	$483.5 \pm 5.0$	$(13.1 \pm 0.6)$	>98	$2.9 \pm 0.6$
Xe	$385.1 \pm 4.0$	$(9.2 \pm 0.8)$	>98	$0.9 \pm 0.2$

the gas and laser pulse. Typical beam profiles using Ar, Kr, and Xe as the carrier gases can be found in Figure 5. From the beam profiles, the mean velocity and longitudinal velocity spread were deduced. The effect of the valve opening time and the laser excitation volume was taken into account for the determination of the longitudinal velocity distribution. To eliminate any influence from the valve opening time, it was reduced until the temporal beam profile did not change any more. The effect of the laser excitation volume has been considered during the fitting procedure of the beam profiles to obtain the velocity distribution. For Ar, Kr, and Xe, the mean velocities of the OH beam are determined as  $670.5 \pm 6.3$  m s<sup>-1</sup>,  $483.5 \pm 5.0$  m s<sup>-1</sup>, and  $385.1 \pm 4.0$  m s<sup>-1</sup>, respectively. The longitudinal velocity spreads are  $(9.8 \pm 0.5)\%$ ,  $(13.1 \pm 0.6)\%$ , and  $(9.2 \pm 0.8)\%$ . The reason for the broader velocity spread using Kr as carrier gas compared to the other carrier gases is not clear, but it is a common observation in all our measurements. Similar observations have been reported previously.<sup>29</sup> The velocity spreads using the present radical source are significantly less than those reported previously.<sup>17,18</sup> The improved beam profile makes the NPV-based discharge source an excellent candidate for deceleration and trapping experiments.<sup>7,25,30–33</sup> Further improvement of the discharge electronics by implementing an active switching-off function would allow an even shorter discharge duration and therefore provides a better definition of the temporal and spatial properties of the generated OH beam.

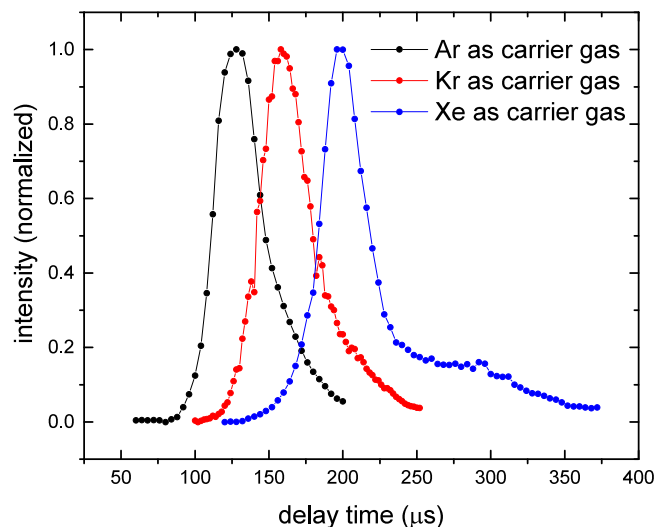


FIG. 5. Temporal profiles of the OH beam generated by the pinhole-discharge for the three carrier gases Ar, Kr, and Xe. The amplitude of the profiles has been normalized for better comparison.

## 2. Rotational state populations

The populations of the rotational states of the OH radicals have been determined by scanning the laser wavelength to cover all transitions from  $J'' = 3/2$  up to  $J'' = 9/2$  level of the electronic ground state  $X^2\Pi(v = 0)$  to the first excited state  $A^2\Sigma(v = 1)$ . Here  $J$  denotes the total angular-momentum quantum number. The rotationally resolved electronic spectrum of OH seeded in Ar is given in Figure 6. The assignment of the spectral peaks is based on the LIFBASE database.<sup>34</sup> The  $P_1(1)$  and  $Q_1(1)$  (and  $Q_{21}(1)$ ) transitions originating from the  $J'' = 3/2$  rotational ground state and  $P_1(2)$  (and  $P_{21}(2)$ ) and  $Q_1(2)$  (and  $Q_{21}(2)$ ) of the first rotationally excited  $J'' = 5/2$  are clearly resolved. Since our dye laser has a bandwidth of about  $0.1 \text{ cm}^{-1}$ , the lines  $Q_1(1)$  and  $Q_{21}(1)$ ,  $P_1(2)$  and  $P_{21}(2)$ , and  $Q_1(2)$  and  $Q_{21}(2)$  are overlapped and not resolvable. By integrating over these spectral features, we conclude that around 98% of the molecules are in the rotational ground state. For the pinhole-discharge source, we find that neither changing the carrier gas nor the backing pressure between 0.5 bars and 5 bars significantly influences the rotational state populations. The large rotational ground state population is a direct result of the optimized shape of our nozzle<sup>24</sup> and the arrangement of the discharge plates. Since the OH radicals are generated at the very front of the nozzle, a large number of collisions can happen to efficiently convert the rotational energy to the translational energy thus to rotationally cool down the OH cloud. The nozzle shape together with the discharge assemblies is also carefully designed to minimize reactions between the radicals before they enter the collision free region.<sup>35</sup>

## 3. OH beam density

The OH beam density can be determined from the absolute number  $N$  of OH molecules in a given detection volume. This number is given by the relation<sup>17</sup>

$$N = \frac{N_{\text{photons}}}{\Omega T Q \epsilon}, \quad (1)$$

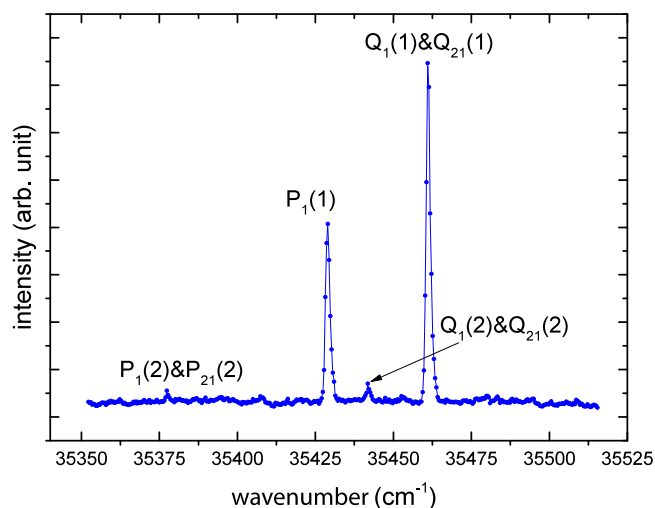


FIG. 6. Rotationally resolved electronic spectrum of OH generated from the pinhole-discharge source. The carrier gas is Ar. The  $P_1(1)$  and  $Q_1(1)$  ( $Q_{21}(1)$ ) transitions from the  $J'' = 3/2$  ground state and the  $P_1(2)$  ( $P_{21}(2)$ ) and  $Q_1(2)$  ( $Q_{21}(2)$ ) from the first rotationally excited state  $J'' = 5/2$  are clearly resolved. The x-axis is the excitation laser wavenumber.

where  $N_{\text{photons}}$  is the number of detected photons for a given transition,  $\Omega$  is the solid angle observed by the PMT,  $Q$  is the quantum efficiency of the PMT,  $T$  is the transmission of the optics, and  $\epsilon$  is the excitation rate factor at saturated detection conditions.<sup>17,36,37</sup> The main challenge in the density measurement is to accurately determine the solid angle for the collection of fluorescence of the detection apparatus and the laser detection volume. To this end, the collection lens has been replaced by two pinholes. The first pinhole has a diameter of 0.2 mm and is placed 5 mm above the laser and OH beam interaction point. The second pinhole with a diameter of 1.0 mm is located directly in front of the PMT. This arrangement allows an accurate definition of the solid angle ( $\Omega = 0.842 \text{ sr}$ ) and the detection volume ( $V = 3.8 \times 10^{-4} \text{ cm}^3$ ). To compensate for the reduction in signal, all light filters have been removed. The contribution of the stray light has been determined to be less than 5%. Measurements are done under saturated conditions where  $\epsilon = 1/3$  for the  $P_1(1)$  transition.<sup>38</sup> Under these conditions, the OH densities 5 cm downstream from the nozzle have been determined to be  $(3.0 \pm 0.6) \times 10^{11} \text{ cm}^{-3}$  for Ar,  $(2.9 \pm 0.6) \times 10^{11} \text{ cm}^{-3}$  for Kr, and  $(0.9 \pm 0.2) \times 10^{11} \text{ cm}^{-3}$  for Xe. These densities exceed the ones obtained with previously used sources by about an order of magnitude<sup>18</sup> and nicely demonstrate the advantages of the NPV for radical production. These features will be particularly beneficial in experiments in which the particle density is crucial, for example, collision, deceleration, and trapping experiments.<sup>4</sup>

## B. DBD source

The same characterization procedure has been carried out for the DBD source. In addition, for some measurements,  $O_2$  molecules have been added to the gas mixture to improve the efficiency of OH production. The main properties of the OH beam thus generated are summarized in Table II and discussed in the following.

The mean velocity and the velocity spread are comparable to the results of the pinhole-discharge source. The DBD source, however, seems to exhibit improved cooling characteristics: we conclude that more than 99% of molecules are in the ro-vibrational ground state, since in the rotationally resolved electronic transition spectrum, no signal due to transitions from  $J'' = 5/2$  can be found within our sensitivity limits as shown in Figure 7. We attribute this improvement to the gentler discharge process in the DBD. These results indicate that the DBD source is preferable when colder species are required.

TABLE II. OH radical beam properties generated from the DBD source.

Carrier gas	Mean velocity /ms <sup>-1</sup>	Velocity spread (FWHM) (%)	Population in rotational ground state (%)	Density $\times 10^{11}$ /cm <sup>-3</sup>
Ar	$646.2 \pm 7.1$	$(11.2 \pm 0.7)$	>99	$1.0 \pm 0.5$
Ar+20%O <sub>2</sub>	$693.8 \pm 7.3$	$(12.8 \pm 1.1)$	>99	$2.6 \pm 0.6$
Kr	$489.9 \pm 5.6$	$(17.2 \pm 1.5)$	>99	$0.9 \pm 0.4$
Kr+16%O <sub>2</sub>	$509.3 \pm 5.9$	...	>99	$2.3 \pm 0.5$
Xe	$396.5 \pm 4.5$	$(12.6 \pm 0.7)$	>99	$0.3 \pm 0.1$
Xe+4%O <sub>2</sub>	$475.0 \pm 5.2$	...	>99	$0.7 \pm 0.3$

However, one may note that the OH density generated by the DBD source is a factor 3 lower for all carrier gases in comparison with the pinhole-discharge source. This is partially caused by the difference in nozzle shape of the two sources. The nozzle diameter of the DBD source is 0.3 mm which is smaller than the 0.5 mm opening of the pinhole-discharge source. The conventional pinhole-discharge valve has a 60° nozzle opening whereas the DBD valve has a 50° cone. These differences may be partly responsible for the different performances of the two valves. Another possible reason is that the chemistry of the plasma generated by the conventional discharge differs significantly from the DBD due to the intrinsically different discharge processes. Generally, we expect the conditions in the DBD to be gentler than in the pinhole-discharge.

Furthermore, we observed that adding O<sub>2</sub> molecules to the water/carrier gas mixture enhances the radical density generated by the DBD source by a factor of around 2.5 as shown in Table II. The discharge process also seems to be more stable with the additional O<sub>2</sub> molecules in the gas mixture. The shot-to-shot noise is reduced to variations of a few percent compared to the results without adding O<sub>2</sub>. Interestingly, a similar performance enhancement was not observed by adding O<sub>2</sub> to the gas mixture in the conventional discharge valve.

Moreover, the mean beam velocity in a supersonic expansion depends on the average mass of the gas mixture. Adding O<sub>2</sub> to the beam changes its average mass and gives us the ability to tune the mean beam velocity by changing the O<sub>2</sub> concentration. For example, we managed to tune the mean velocity of the OH beam from 510 m s<sup>-1</sup> to 495 m s<sup>-1</sup> by varying the concentration of oxygen between 40% and 10% in Kr without noticeable loss in the OH density. This provides additional flexibilities for experiments, in which the velocity of the incoming molecular beam plays a significant role, like Stark deceleration experiments.<sup>39</sup>

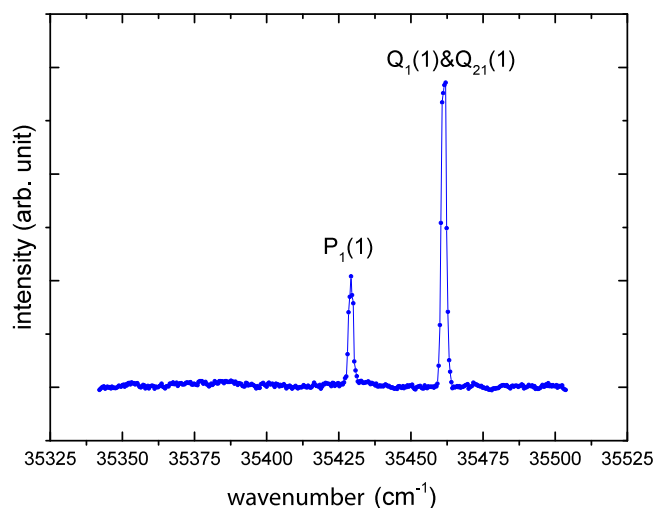


FIG. 7. Rotationally resolved electronic spectrum of OH generated from the DBD source. The carrier gas is Ar. The P<sub>1</sub>(1) and Q<sub>1</sub>(1) (Q<sub>2</sub>(1)) transitions from the J'' = 3/2 ground state are observed. No indication of the P<sub>1</sub>(2) and Q<sub>1</sub>(2) transition from the first excited rotational state J'' = 5/2 can be found. The x-axis is the excitation laser wavenumber.

## IV. CONCLUSIONS

We presented two high-performance discharge sources which provide an efficient and reliable method to generate cold and intense beams of free radicals for many kinds of experiments. We have shown that combining state-of-the-art discharge technology with the high-density and short-pulse Nijmegen pulsed valve enables the creation of high-quality OH beams. Both the conventional pinhole-discharge and the DBD sources show excellent beam properties in comparison to previous sources. We note that other advanced radical sources, e.g., DBDs coupled with Even–Lavie valves,<sup>23</sup> may give a comparable performance. However, no direct comparison has been made yet. Both implementations succeed in the creation of a translationally cold, rotationally cold, and intense OH radical beam. The gentle nature of the discharge process in the DBD source results in a ground state population exceeding 99%. The large density and low translational temperature will benefit deceleration and trapping experiments. For the DBD source, addition of O<sub>2</sub> to the gas mixture increases the OH radical density and discharge stability and allows to tune the mean beam velocity. Both sources still provide room for further improvement, for example, a better designed nozzle shape adapted to the discharge parts and upgraded electronics to generate more stable and better defined discharge process. Second generations of both radical sources are already under construction in our lab.

## ACKNOWLEDGMENTS

We acknowledge financial support from the Swiss National Science Foundation and the University of Basel. We thank Professor Jun Ye (Boulder) for kindly providing us the construction drawings of his pinhole-discharge source. We also thank D. Wild, Ph. Knöpfel, G. Martin, and N. Janssen for their excellent technical support. S.Y.T.v.d.M. acknowledges financial support from the European Research Council via a Starting Grant and support from the Netherlands Organization for Scientific Research. L.P. acknowledges financial support from the Beyond the Frontiers Programme of the Radboud Honours Academy.

- <sup>1</sup>J. C. Whitehead, *Rep. Prog. Phys.* **59**, 993 (1996).
- <sup>2</sup>K. Liu, R. G. Macdonald, and A. F. Wagner, *Int. Rev. Phys. Chem.* **9**, 187 (1990).
- <sup>3</sup>*Handbook of High-Resolution Spectroscopy*, edited by M. Quack and F. Merkt (John Wiley & Sons, New York, 2011).
- <sup>4</sup>M. Brouard, D. H. Parker, and S. Y. T. van de Meerakker, *Chem. Soc. Rev.* **43**, 7279 (2014).
- <sup>5</sup>B. K. Stuhl, M. T. Hummon, and J. Ye, *Ann. Rev. Phys. Chem.* **65**, 501 (2014).
- <sup>6</sup>J. Jankunas and A. Osterwalder, *Ann. Rev. Phys. Chem.* **66**, 241 (2015).
- <sup>7</sup>S. Y. T. van de Meerakker, H. L. Bethlem, N. Vanhaecke, and G. Meijer, *Chem. Rev.* **112**, 4828 (2012).
- <sup>8</sup>Y.-P. Chang, D. A. Horke, S. Trippel, and J. Küpper, *Int. Rev. Phys. Chem.* **34**, 557 (2015).
- <sup>9</sup>M. B. May, T. Aung-Htut, A. Ayer, and I. W. Dawes, "Oxidative stresses and ageing," in *Aging Research in Yeast*, edited by P. Laun, M. Breitenbach, and S. M. Jazwinski (Springer, Dordrecht, Netherlands, 2012), pp. 13–54.
- <sup>10</sup>M. M. Litvak, A. L. McWhorter, M. L. Meeks, and H. J. Zeiger, *Phys. Rev. Lett.* **17**, 821 (1966).
- <sup>11</sup>F. J. Comes, *Angew. Chem., Int. Ed.* **33**, 1816 (1994).
- <sup>12</sup>M. Blocquet, C. Schoemaeker, D. Amedro, O. Herbinet, F. Battin Leclerc, and C. Fittschen, *Proc. Natl. Acad. Sci. U. S. A.* **110**, 20014 (2013).

- <sup>13</sup>P. Andresen, N. Aristov, V. Beushausen, D. Häusler, and H. Lülf, *J. Chem. Phys.* **95**, 5763 (1991).
- <sup>14</sup>J. W. Farthing, I. W. Fletcher, and J. C. Whitehead, *J. Phys. Chem.* **87**, 1663 (1983).
- <sup>15</sup>J. J. ter Meulen, W. Meerts, G. Van Mierlo, and A. Dymanus, *Phys. Rev. Lett.* **36**, 1031 (1976).
- <sup>16</sup>M. C. van Beek and J. J. ter Meulen, *Chem. Phys. Lett.* **337**, 237 (2001).
- <sup>17</sup>K. Ikejiri, H. Ohoyama, Y. Nagamachi, T. Teramoto, and T. Kasai, *Chem. Phys. Lett.* **379**, 255 (2003).
- <sup>18</sup>H. Lewandowski, E. R. Hudson, J. Bochinski, and J. Ye, *Chem. Phys. Lett.* **395**, 53 (2004).
- <sup>19</sup>U. Kogelschatz, *Plasma Chem. Plasma Process.* **23**, 1 (2003).
- <sup>20</sup>U. Kogelschatz, B. Eliasson, and W. Egli, *Pure Appl. Chem.* **71**, 1819 (1999).
- <sup>21</sup>M. B. Chang and C. C. Lee, *Environ. Sci. Technol.* **29**, 181 (1995).
- <sup>22</sup>B. Gellert and U. Kogelschatz, *Appl. Phys. B* **52**, 14 (1991).
- <sup>23</sup>K. Luria, N. Lavie, and U. Even, *Rev. Sci. Instrum.* **80**, 104102 (2009).
- <sup>24</sup>B. Yan, P. F. H. Claus, B. G. M. van Oorschot, L. Gerritsen, A. T. J. B. Eppink, S. Y. T. van de Meerakker, and D. H. Parker, *Rev. Sci. Instrum.* **84**, 023102 (2013).
- <sup>25</sup>S. N. Vogels, Z. Gao, and S. Y. van de Meerakker, *EPJ Tech. Instrum.* **2**, 12 (2015).
- <sup>26</sup>K. Luria, W. Christen, and U. Even, *J. Phys. Chem. A* **115**, 7362 (2011).
- <sup>27</sup>C. W. Bauschlicher and S. R. Langhoff, *J. Chem. Phys.* **87**, 4665 (1987).
- <sup>28</sup>D. R. Yarkony, *J. Chem. Phys.* **97**, 1838 (1992).
- <sup>29</sup>R. T. Jongma, "Molecular beam experiments and scattering studies with state-selected metastable CO," Ph.D. thesis (Radboud University Nijmegen, 1997).
- <sup>30</sup>S. Y. T. van de Meerakker, N. Vanhaecke, M. P. J. van der Loo, G. C. Groenenboom, and G. Meijer, *Phys. Rev. Lett.* **95**, 013003 (2005).
- <sup>31</sup>N. Vanhaecke, U. Meier, M. Andrist, B. H. Meier, and F. Merkt, *Phys. Rev. A* **75**, 031402 (2007).
- <sup>32</sup>E. Narevicius, C. G. Parthey, A. Libson, J. Narevicius, I. Chavez, U. Even, and M. G. Raizen, *New Journal of Physics* **9**, 358 (2007).
- <sup>33</sup>K. Dulitz, A. Tauschinsky, and T. P. Softley, *New Journal of Physics* **17**, 035005 (2015).
- <sup>34</sup>J. Luque and D. Crosley, SRI International Report MP, 99, 1999.
- <sup>35</sup>S. Willitsch, J. M. Dyke, and F. Merkt, *Helvetica chimica acta* **86**, 1152 (2003).
- <sup>36</sup>D. R. Guyer, L. Hüwel, and S. R. Leone, *J. Chem. Phys.* **79**, 1259 (1983).
- <sup>37</sup>J. M. Hossenlopp, D. T. Anderson, M. W. Todd, and M. I. Lester, *J. Chem. Phys.* **109**, 10707 (1998).
- <sup>38</sup>R. Altkorn and R. N. Zare, *Annu. Rev. Phys. Chem.* **35**, 265 (1984).
- <sup>39</sup>D. Zhang, G. Meijer, and N. Vanhaecke, *Phys. Rev. A* **93**, 023408 (2016).